PHYSICAL REVIEW A VOLUME 2, NUMBER 5 NOVEMBER 1970

Vibrational Excitation by Electron Impact in O_2[†]

D. Spence and G. J. Schulz
Mason Laboratory, Yale University, New Haven, Connecticut 06520
(Received 22 April 1970)

The trapped-electron method is applied to a study of vibrational excitation by low-energy (0–1-eV) electrons on O_2. It is found that the dominant feature of the vibrational cross section consists of spikes, spaced about 0.11 eV apart. This spacing is characteristic of the spacing of the vibrational levels of the O_2^- system which serves as a compound state and which is also measured in the present study. It is found that one of the levels of the compound system (O_2^-) is coincident with the $v=3$ level of O_2. When the measured anharmonicity of the O_2^- system (3 ± 0.5 mV per level) is taken into account, the spacing of the lowest vibrational states ($v'=0\rightarrow v'=1$) of O_2^- becomes 132 mV, provided that the Pack-Phelps value of 0.43 eV is used for the electron affinity of O_2. The spacing of the $v'=0\rightarrow v'=1$ vibrational states obtained in the present experiment is in excellent agreement with the values obtained by Raman spectroscopy of alkali-halide crystals in which O_2^- is trapped (135 mV). The magnitudes of the cross sections of the spikes, integrated over the electron energy distribution, are given and the branching ratio for the decay of O_2^- states is discussed.

I. INTRODUCTION

This paper presents the results of measurements of elastic and inelastic processes occurring in oxygen at incident electron energies below 1 eV. Specifically, the measurements are undertaken in order to clarify the processes by which vibrational excitation of the oxygen molecule occurs.

Vibrational excitation of diatomic molecules can occur by two different processes; namely, by "direct" excitation of the vibrations, and by excitation of a compound (temporary negative ion) state,[1] and subsequent decay into a free electron plus a neutral vibrationally excited molecule. In diatomic molecules, excitation via a compound state is often the dominant process by which vibrational excitation of the neutral molecule occurs. These processes have been studied[2,3] in N_2, H_2, and CO, and in all these molecules it is found that excitation via the compound state is dominant in the energy range over which the compound state is formed. In H_2 the compound state is located around 2 eV, and its width[4] is several eV. Because of this large width, the concept of the compound state begins to break down in some ways, but it retains its utility for an understanding and a prediction of vibrational excitation and dissociative attachment. In N_2 and CO the compound states are located around 2.3 and 1.7 eV, respectively, and the average widths are narrower than in H_2 (about 0.2 eV). In all the above cases, the molecule does not form a stable parent negative ion.

The oxygen molecule presents a new and interesting system by virtue of the fact that O_2 forms a stable negative ion. It can therefore be expected that the existence of the O_2^- potential-energy curve[5] in the Franck-Condon region of O_2 provides, automatically, a compound state which can be effective in the process of vibrational excitation at low electron energies. An added inducement for the study of the O_2 system is provided by the estimate of the lifetime of the compound state, which is much longer[6] (about 10^{-10} sec) than the compound states studied previously.

Very few data are available concerning vibrational excitation of the oxygen molecule by electron impact. An electron-beam experiment concerning vibrational excitation in O_2 was performed by Schulz and Dowell,[7] who measured the cross sections at a fixed electron energy (0.16 eV) above the threshold of vibrational excitation. Although their experiment was not sufficiently detailed to establish clearly the mechanisms involved, they pointed out that the vibrational cross section of O_2 can be expected to consist of a series of spikes at the position of the vibrational levels of O_2^-. However, direct excitation could not be excluded as an additional process.

Hake and Phelps[8] performed an analysis of transport coefficients to obtain a set of vibrational cross sections in O_2. In an attempt to make their analysis compatible with the beam experiment of Schulz and Dowell, they postulated that the vibrational cross sections to various states consist of a "direct" component which rises slowly with energy and a "compound-state" component consisting of a spike at the position of the nearest compound state. The "spikes" were placed about 0.19 eV apart. This spacing of the spikes enabled Hake and Phelps to make the magnitude of the cross section observed in the beam experiment consistent with the magnitude of the cross sections needed for the transport coefficients by assuming that the small magnitude of the cross section derived from the electron-beam experiment is characteristic of the "direct" com-

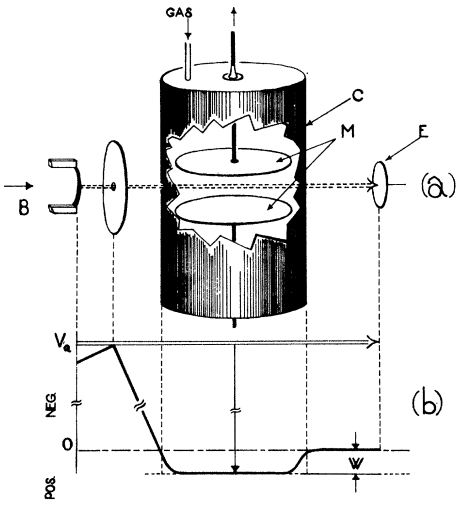

FIG. 1. Schematic diagram of the tube and the potential distribution along the axis of the electron beam.

ponent and that the "compound-state" component has not been included in the electron-beam experiment.

We show in this paper that some of the assumptions leading to the analysis described above need to be reconsidered in the light of the present experiment. We do confirm that the vibrational excitation consists of a "direct" component and a series of spikes. We find, in agreement with Boness and Hasted, [9] that the spacing of the vibrational levels in O_2^- is about 0.11 eV, and we also find that the spacing of the "spikes" in the vibrational cross section is 0.11 eV. We confirm the magnitude of the cross section found by Schulz and Dowell, and we attribute the magnitude to the reaction proceeding via specific compound states. We find that compound states (O_2^-) show a preference for decay into the lowest vibrational states of the molecule; i.e., there is a preference for emitting electrons with the highest kinetic energy. This aspect of the collision process has not been included in the analysis of Hake and Phelps.

II. EXPERIMENT

Figure 1 is a schematic diagram of the experimental tube employed in the present studies. This tube has been described in detail previously, [10] and only a brief review will be given here. For the present studies, the tube is used in a different mode of operation than the mode used in the past.

Electrons are emitted from a directly heated thoria-coated iridium filament (F) whose effective energy distribution is reduced to about 60–70 meV by the retarding-potential-difference method. [11] The electron beam is confined by a magnetic field (B) which can be varied from zero to about 2500 G. The collision chamber consists of an iridium cylinder (C) inside of which is mounted a pair of parallel iridium plates (M) which serve as collectors. All electrodes, with the exception of the iridium parts and the primary electron-beam collector, are gold plated to minimize contact potential differences. After baking at 400 °C for 24 h, the background pressure in the vacuum system is of the order of 2×10^{-9} Torr. The gas pressure in the collision chamber is varied between 10^{-5} and 2×10^{-3} Torr.

For measurements of inelastic processes, the trapped-electron method [12,13] is used. This method has a high sensitivity for the study of inelastic processes because all electrons which have made inelastic collisions are collected and measured. A detailed description of the trapped-electron method has been given previously, [12,13] and only the main points of the method will be given here.

The method consists of trapping low-energy electrons in an electrostatic well and collecting them with high efficiency. For clarity, the nomenclature used here is the same as that used in Ref. 12. When a positive potential is applied to the collector M with respect to the collision chamber C, a potential well (W) is formed in the collision chamber, as shown in Fig. 1(b) where the potential distribution along the axis of the tube is plotted. The potential difference between electrodes P and C is denoted by V_a in Fig. 1(b), and it can be seen that the electron energy in the collision chamber is $e(V_a+W)$. The energy of the electrons as a function of position is indicated by the double horizontal line of Fig. 1(b). When electrons in the beam lose nearly all their energy in an inelastic collision, as they do when the incident electron energy is just above the threshold of excitation, they will end up in the potential well from which they cannot escape. These electrons will eventually migrate to the collector M where they are measured. Electrons which have lost energy less than (eV_a) are not trapped and can reach the electron-beam collector or the collision-chamber walls.

New Methods for Evaluation of Data

In the past it has been customary to plot the trapped-electron current at a fixed well depth W as a function of electron accelerating voltage. Below, we describe how the data obtained by the trapped-electron method can be handled to give information regarding the shape of the excitation function near threshold; this new method is particularly useful when sharp structure in the inelastic cross section is present.

For an excitation function which increases monotonically with energy above its threshold eV_x, the electron current (measured at the collector M) has an onset at an energy $E=eV_x$ and a maximum at E

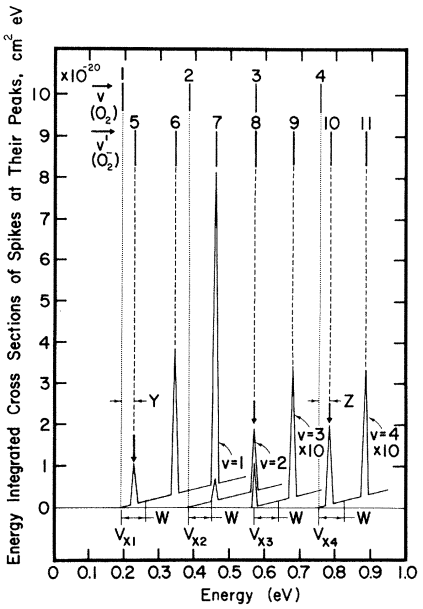

FIG. 2. Shape of cross sections for vibrational excitation in O_2. The shapes are consistent with the results of the present experiment, but the resolution is insufficient to specify the width of the spikes resulting from the compound states or to determine accurately the slowly rising background which constitutes the "direct component." The energy integrated cross section at the peaks is given on the ordinate. Note that the curves for $v=3$ and $v=4$ are multiplied by a factor of 10 in order to make them more easily visible. The branching ratio for the decay of $O_2^-(v'=8)$ into $O_2(v=2)$ and O_2 $(v=3)$ is 17.

$= e(V_x + W)$. A plot of the trapped-electron current versus electron accelerating voltage exhibits a spacing between trapped-electron peaks which is equal to the spacing of the vibrational levels. A plot of the energy in the collision chamber at which a given trapped-electron peak occurs, versus the well depth, is a straight line with an intercept at the threshold energy and a slope of unity. It should be emphasized that whatever the shape of the excitation function, the magnitude of the trapped-electron current will follow the shape of the excitation function up to W above threshold as the electron energy is increased. For $V_a > V_x$, the trapped-electron current drops to zero.

Let us now consider another case. Figure 2 shows a set of vibrational excitation functions. These are in fact characteristic of the excitation functions in O_2, and the justification for them will be given later in the paper. They consist of a slowly rising "direct" component and a sharp "resonance" contribution, analogous to the excitation function proposed by Hake and Phelps.[8] In this case the separation of the experimentally measured trapped-electron peaks need not equal the separation of the vibrational levels of the O_2 molecule. The maxima of the trapped-electron peaks occur at the positions of the spikes, provided that the separation between the first spike of a given excitation function and its threshold is less than the well depth W. In this case, a plot of the energy at which the maximum of the trapped-electron peak occurs versus well depth remains independent of well depth. If this spike occurs at energies higher than the well depth, the maximum of the trapped-electron peak occurs at $e(V_x + W)$, and we have the situation described in the preceding paragraph. Thus, for a trap of depth W, the assumed set of cross sections of Fig. 2 leads to trapped-electron peaks at absolute energies $e(V_{x_1} + y)$, $e(V_{x_2} + W)$, eV_{x3}, and $e(V_{x_4} + z)$. The symbols y and z represent the spacing of the spikes from the respective threshold and are defined in Fig. 2.

If the resolution of the electron beam is high compared to the widths and separation of the spikes, then the exact shape of the cross section up to W above threshold would be measured. However, the resolution of the present apparatus is comparable to the separation of the spikes and we can extract information only with regard to the position and the magnitude of the trapped-electron peaks. Nevertheless, we are able to resolve separate spikes of a given excitation function when the well depth is deep enough to encompass more than one spike of such an excitation function. When the trap is deeper than the separation of vibrational states of the O_2 molecule, the interpretation of the data is extremely difficult. In this case there are contributions to the trapped-electron current from more than one excitation function at some incident electron energies.

In the energy region of interest in O_2 (0–1 eV) it is possible for elastically scattered electrons to be trapped and to reach the collector. This process has been described in detail previously[13] and gives rise to an electron peak at zero energy which decreases monotonically and disappears at 1–1.5 eV. Thus all the inelastic structure below 1 eV is superimposed on an elastically scattered background current. In the present apparatus this elastic background is much smaller than the inelastic structure, which greatly simplifies analysis of the data. The reduction of the elastically scattered background current has been discussed by Burrow *et al.*[13] Undoubtedly, the elimination of grids in the collision chamber of the present apparatus is beneficial.

In the energy region 0–1 eV it is also possible to form stable O_2^- by three-body attachment. Because the gas pressure used in the present experiment is low, the contribution from O_2^- to the measured current is entirely negligible.

In the present experiments, two methods of data acquisition are used. The first is an ac method

using phase-sensitive detection of the signals. The second is a dc method in which the signal is measured by a vibrating-reed electrometer and stored in a multichannel analyzer. The analyzer is used as a signal averager for multiple scans of the electron energy. The potential on the retarding electrode of the electron gun and the add/subtract circuit of the multichannel analyzer are switched at the beginning of alternate scans, in a mode similar to that described by Chantry,[14] to give automatic data recording.

The primary electron-beam current is between 5×10^{-9} and 10^{-10} A. When determination of the absolute energies of the trapped-electron peaks is desired, we use the lowest possible values of electron current because the zero-energy peak which serves as an energy reference is most easily affected by space charge.

The well depth is determined by measuring the trapped-electron current produced from the excitation of the 2^3S state in helium, whose shape and magnitude are known, and by normalizing to the positive-ion current in He at 18 eV. This method for determining the effective well depth has been used previously.[13]

III. VIBRATIONAL SPACING OF O_2^- SYSTEM

The vibrational spacing of the O_2^- state has been determined in a subsidiary experiment by studying resonances in the scattering of electrons from oxygen. It is believed that the state involved has a designation $^2\Pi_g$ and is the ground electronic state of O_2^-. Boness and Hasted[15] used a transmission method in which the structure in the total transmitted current was examined. Boness and Schulz[16] studied the elastically scattered electrons alone using a double electrostatic analyzer. Both measurements give the vibrational spacing of the O_2^- $^2\Pi_g$ state to be about 0.11 eV. This value has been confirmed in the present experiment using the apparatus described in Sec. II. The present results give not only the vibrational spacings, but also the anharmonicity of the vibrational levels of the O_2^- $^2\Pi_g$ state.

For the measurement of the elastic cross section, the potential well is reduced to zero so as not to trap electrons from inelastic processes. The magnetic field is reduced to the lowest value that will still collimate a useful beam, about 20–30 G. Under these conditions, some of the electrons which are elastically or inelastically scattered in the collision chamber are able to reach the collector M. This is verified by observations of the resonance in helium[17] at 19.3 eV. It must be remembered that this mode of operation differs from the trapping of electrons in a potential well.

Figure 3 is a typical recorder tracing of scattered current from O_2 as a function of electron energy.

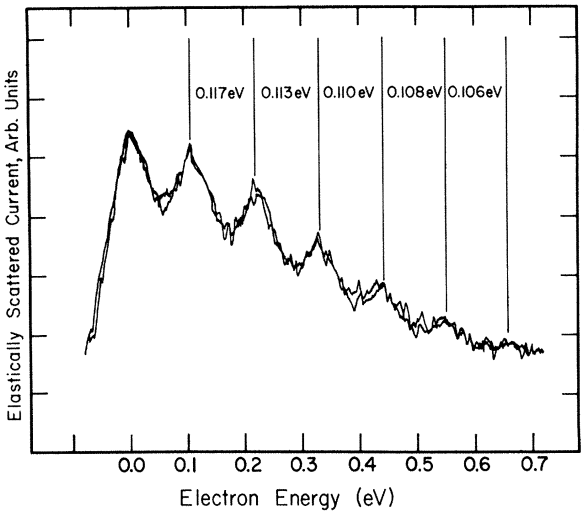

FIG. 3. Recorder tracing of the scattered current as a function of electron energy. The structure, representing a variation of about 10% of the total current, is interpreted as the resonance contribution to the elastic cross section. The spacing of the peaks, indicated in the figure, corresponds to the spacing of the vibrational levels ($v'=4-9$) of O_2^- $^2\Pi_g$.

The zero has been suppressed for greater clarity and the structure represents a variation of about 10% of the total current. We attribute the structure observed in Fig. 3 to elastically scattered electrons, because we find that the inelastic cross sections are at least an order of magnitude smaller than the elastic cross sections.[17]

Boness and Schulz[16] were not able to observe the vibrational cross sections in O_2, although they could observe the structure in the elastic cross section with a signal-to-noise ratio of about 20:1. This negative experiment also indicates that the inelastic cross sections via the compound state in O_2 are at least an order of magnitude smaller than the resonances in the elastic cross section.

The spacing of the peaks in Fig. 3 can be measured to 2–3-mV accuracy. The anharmonicity is seen to be 3 ± 0.5-mV per level. Any value of anharmonicity outside these limits would clearly not fit the present data compounded over six vibrational levels of the negative ion. The spacing of the first two peaks of Fig. 3 is ignored, as the first peak is due to scattering of zero-energy electrons and is not necessarily associated with a resonance.

IV. INELASTIC MEASUREMENTS IN O_2 BELOW 1 eV

Figure 4 shows a series of plots of trapped-electron current versus electron energy, V_a+W, at various well depths. The plots in Fig. 4 are representative of about 100 curves taken. The curves consist of an elastic peak with a superposition of

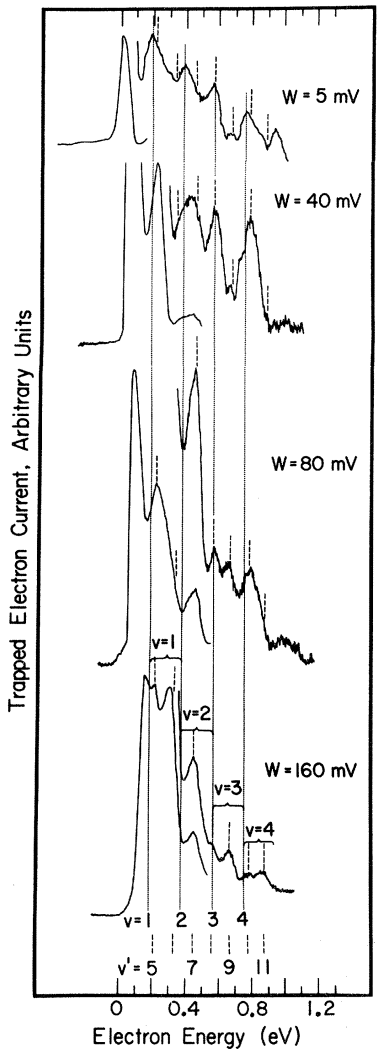

FIG. 4. Trapped-electron current versus electron energy at well depths of 5, 40, 80, and 160 mV. At low well depth, the trapped-electron peaks occur at the position of the vibrational levels of the neutral O_2 $^2\Sigma_g^-$ state marked $v = 1, 2, 3, 4$. At intermediate well depths, the peaks shift on the energy scale. At the higher well depths the peaks occur at the positions of the compound states O_2^-. The positions of the compound states are marked by the dashed vertical lines ($v' = 5 - 11$). At the highest well depth ($W = 160$ mV), the well depth encompasses up to two compound states and the peaks split into doublets. The trapped-electron peak corresponding to $v = 3$ does not shift and this is taken to indicate that there is coincidence between the levels $v = 3$ of O_2 and $v' = 8$ of O_2^-.

inelastic peaks on a monotonically decreasing background current. It is seen that the elastic peak moves to higher energies as the well depth is increased. This is a result of our choice of plotting on the abscissa the energy, $E = V_a + W$ (rather than the accelerating voltage V_a, as was done in previous work). The elastic peak occurs at an accelerating voltage, $V_a = 0$, and thus appears at an energy W.

The absolute energies at which the trapped-electron peaks occur can be obtained either by reading the position of the peak on the energy scale or by measuring the distance between an inelastic peak and the elastic peak and adding the well depth.

Examination of Fig. 4 shows the following interesting features: (a) At the lowest well depth, $0 < W \lesssim 5$ mV, the spacing of the inelastic peaks corresponds to the spacing of the vibrational levels in the neutral molecule, which are indicated by the vertical dotted lines marked $v = 1, 2, 3, 4$. (b) At higher well depth, the spacing of the peaks is different from the vibrational spacing of O_2. The most exaggerated case is seen for a well depth of 80 mV in Fig. 4. Here the spacing between the second and third inelastic peak is 110 mV, not 189 mV as in the ground electronic state. (c) The ratios of the peak heights change as a function of well depth. (d) At the higher well depths, some of the peaks split into doublets.

Peak Height versus Well Depth

In order to interpret curves such as those shown in Fig. 4, the data are replotted in two different ways (see Figs. 5 and 7). Figure 5 shows a plot of the maximum peak height at the indicated well depths. It is seen that the peak height corresponding to $v = 1$, $v = 2$, and $v = 4$ shows three distinct regimes. First, the cross section increases slowly; second, there is a rapid increase in the cross section, and finally, there is a region of "saturation." When the ordinate is multiplied by the factor 10^{-20}, an effective cross section in units of cm^2 can be obtained. Past the point of saturation, the curve does not represent the cross section at the given well depths, but rather the maximum cross section within the indicated well depth. The data of Fig. 5 are completely consistent with the plot of Fig. 2. The regime of slowly increasing cross sections is due to direct excitation of the vibrational modes of O_2. The rapidly rising part of the cross section occurs when the trap starts encompassing the compound state nearest to the vibrational level. The excitation then occurs via the compound state, but the slope of the excitation cross section is due to the finite electron energy distribution. The peak height reaches "saturation" when the whole of the electron energy distribution overlaps the resonant state. Also shown in Fig. 5 is the peak height of the trapped-electron signal when the respective peak splits into a doublet at higher well depth. This splitting occurs (for $v = 1$ and $v = 3$) when the well depth is large enough to encompass two compound states.

The curve for $v = 3$ differs markedly from the curves for $v = 1, 2$, and 4 in that there is no change in slope at low well depths; it rises at onset and then saturates. We interpret this behavior as an indication that the compound state is almost coin-

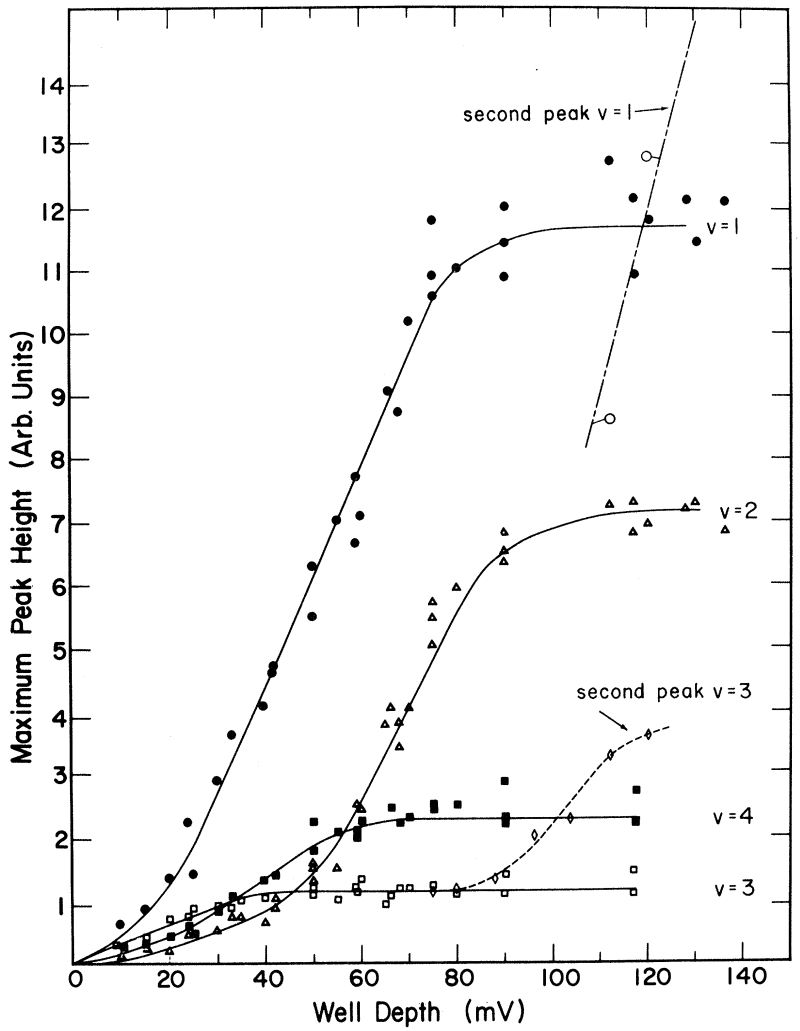

FIG. 5. Maximum peak height at the well depth indicated on abscissa. Multiply ordinate by 10^{-20} to obtain approximate effective cross section in cm^2. At the highest well depths, peaks split into doublets. This is indicated by the lines second peak for $v=1$ and $v=3$.

cident with (or slightly above) the vibrational level $v=3$. This observation represents one of the important results of this experiment, and will be further substantiated in connection with the discussion of Fig. 7. The coincidence in energy between the $v=3$ vibrational state of O_2 and one of the vibrational states of O_2^- fixes the relative positions of the vibrational levels of the two systems.

Energy Levels of O_2^-

Coupled with our knowledge of the spacing of vibrational levels of O_2^- (see Sec. III), we can plot Fig. 6, which shows the relative positions of vibrational levels of[18] O_2 and of O_2^-. The anharmonicity of O_2^- is included. We stop the progression of vibrational states at the quantum nearest the known value of the electron affinity of O_2. Although several values of electron affinity are being quoted,[19,20] examination of the experimental evidence indicates to us that at this time only the value of Pack and Phelps[21] is free from serious objection and thus we take this value, 0.43 eV, as the electron affinity of O_2.

Figure 6 clearly indicates that two vibrational levels of O_2^- (compound states) exist in the interval between the $v=1$ and $v=2$, the $v=3$ and $v=4$, and also between the $v=4$ and $v=5$ states of O_2. As the well is increased in depth, it will eventually be deep enough to encompass two compound states for vibrational excitation for $v=1$, $v=3$, and $v=4$. Our model, shown in Fig. 6, shows that this overlap with the second compound state occurs first for $v=3$. This is verified by examination of Fig. 4, which shows that at the larger well depth the peaks corresponding to vibrational excitation of $v=3$, $v=4$, and $v=1$ are split, each peak corresponding to vibrational excitation via a different compound state. This effect is also shown by the dashed lines in Fig. 5, which show the behavior of the second peak causing vibrational excitation to $v=1$ and $v=3$ as a function of well depth. The second peak to $v=3$ appears at lower well depth than the second peak for $v=1$, consistent with our model of Fig. 6.

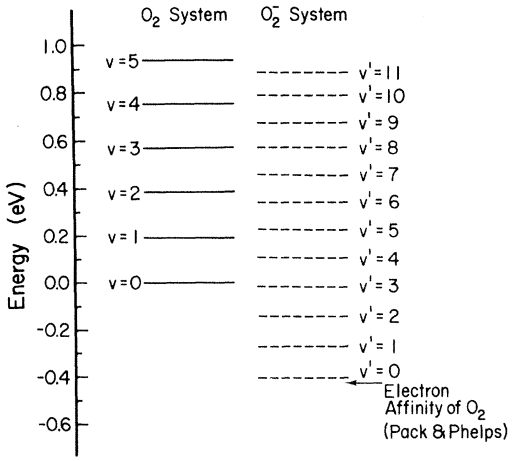

FIG. 6. Vibrational levels of $O_2\ ^3\Sigma_g^-$ and $O_2^-\ ^2\Pi_g$. The vibrational spacing of the ground electronic state of O_2 comes from Ref. 18, and the vibrational spacing as well as the anharmonicity of O_2^- have been measured in the present experiment. The ladder of O_2^- is fixed with respect to the ladder for O_2 by noting the coincidence between level $v=3$ in O_2 and $v'=8$ in O_2^-. The downward progression of the O_2^- ladder is stopped at the quantum nearest the electron affinity of O_2. The value of Pack and Phelps (Ref. 21) (0.43 eV) is used for the electron affinity. Extrapolation of the vibrational levels leads to a spacing of 132 mV (1065 cm^{-1}) for $v'=0 \rightarrow v'=1$, in good agreement with the value deduced by Raman spectroscopy of alkali halides in which O_2^- is trapped (see Ref. 25).

Position of Peaks on Energy Scale

Additional, and in some ways more convincing, evidence for the hypothesis that the vibrational excitation functions for O_2 consist of a series of spikes whose spacing is determined by the vibrational levels of O_2^-, can be obtained from Fig. 7. Figure 7 is a plot of the absolute energy at which the trapped-electron peaks occur versus well depth. Also shown on the figure are the locations of the vibrational levels of O_2 (solid horizontal lines) and O_2^- (dashed lines) as determined in Fig. 6. If vibrational excitation proceeds via a direct process, the peak of the trapped electron occurs at an energy $E=V_x+W$ (see Sec. I). Such a process exhibits itself on Fig. 7 as a straight line with intercept at the threshold, V_x, and a slope of unity. Figure 7 shows that such is the case, at low well depth, for $v=1$, 2, and 4. Alternately, if vibrational excitation proceeds via a compound state, the maximum of the trapped-electron current remains at a constant energy which is the energy of the respective compound state. This is seen to be the case at intermediate and high well depth for $v=1, 2$, and 4. It is gratifying to note that the experimental points at intermediate well depth actually lie on the line indicating the location of the compound states. For $v=3$, the peak remains at a constant energy even at low well depths, indicating that the compound state must be located in coincidence (within ~0.01 eV) with $v=3$ of O_2. Figure 7 thus can be taken as a confirmation for our hypothesis that there is a coincidence between one of the levels of the compound system and $v=3$ of O_2. Figure 7 in fact provides an alternative method for determining the relative position of the vibrational levels of the $O_2^-\ ^2\Pi_g$ system.

At large well depth, the trapped-electron peaks become doublets. At these well depths, two levels of the compound system are encompassed. Figure 7 shows the location on the energy scale of the split peaks for $v=1$, $v=3$, and $v=4$ proceeding via $v'=6$, $v'=9$, and $v'=11$, respectively.

V. MAGNITUDE OF CROSS SECTIONS

Absolute cross sections for vibrational excitation of O_2 are determined by comparing the trapped-electron currents with the peak of the dissociative attachment cross section at 6.7 eV. The cross section at the peak for dissociative negative-ion formation[22–24] is taken to be 1.30×10^{-18} cm^2. For negative-ion collection, a field is applied across plates M such that all negative ions formed are collected. The magnitude of the vibrational cross sections determined in this manner can be obtained by multiplying the scale of Fig. 5 by 10^{-20} cm^2. It should be noted that the value of the effective cross sections determined in this experiment at 160 mV above threshold are consistent with the values previously determined by Schulz and Dowell.[7] Because of the expected narrowness of the spikes (< 1 meV) in the cross sections, the only meaningful measurements of their sizes are their energy-integrated cross sections. These are given in Fig. 2. Although Fig. 2 was presented as an assumed set of cross sections, experiment verifies that it is conceptually correct insofar as the locations of the spikes and their relative magnitudes are concerned. However, Fig. 2 is somewhat arbitrary with respect to the widths of the spikes, which have been drawn 10 mV wide for clarity, and with respect to the magnitude of the "direct" component. The magnitude of this "direct" component cannot be determined accurately because it is not easy to extract from Fig. 5 the effect of "tailing" of the electron energy distribution from the direct portion of the cross sections. It must be emphasized that in Fig. 2 the energy-integrated cross-section scale only refers to the spikes at their peaks. This scale is estimated to be correct within 50%. The magnitudes of the spikes are also tabulated in Table I.

VI. DISCUSSION

It has been shown in this paper that the vibrational cross sections of the O_2 system consist of a

series of spikes, coincident with the spacing of the vibrational levels of the $O_2^{-2}\Pi_g$ system.

Since it was not realized previously that the vibrational spacings of the O_2^- system were much less than those of the neutral molecule, Schulz and Dowell were unable to determine whether the excitation they observed at 160 meV above threshold proceeds by a direct process or via a compound state. The present data show that at 160 meV above threshold, the compound state dominate the excitation function. The anomalous average spacing of about 0.2 eV observed by Schulz and Dowell results from the fact that they were not able to resolve the separate spikes of excitation functions,

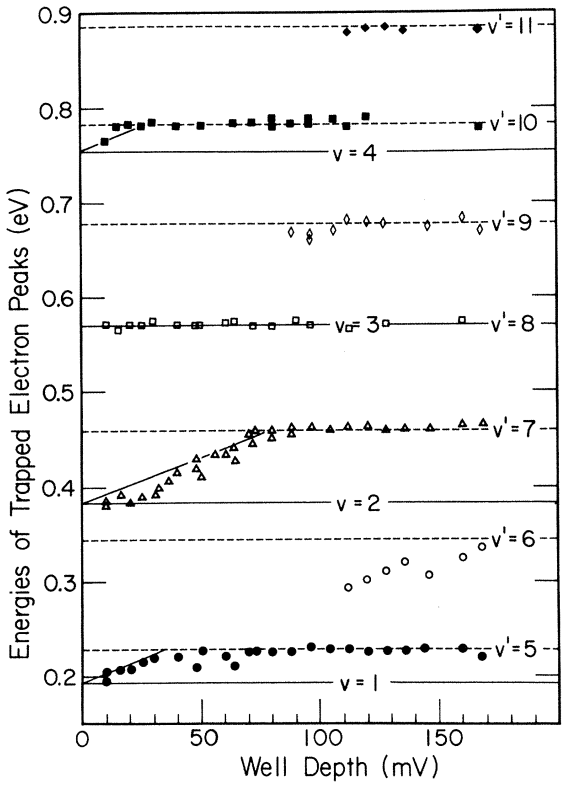

FIG. 7. Absolute energy at which trapped electron peaks occur versus well depth. The solid horizontal lines are the vibrational states of the ground electronic state of $O_2 X^3\Sigma_g^-$ and the dashed horizontal curves are the vibrational levels of the O_2^- $^2\Pi_g$ system. The energy scale and the locations for the horizontal lines are taken from Fig. 6. At intermediate well depth, vibrational excitation proceeds via compound states and the trapped-electron peaks should be located at the position of the compound states determined from Fig. 6. To the extent that the experimental points lie on the horizontal lines for $v' = 5 - 10$, this constitutes an independent determination of the locations of the compound states. At the highest well depths, the trapped-electron peaks split into doublets. The symbols ○, ◇, and ◆ indicate the second peak leading to vibrational excitation of $v = 1$, 3, and 4 via $v' = 6$, 9, and 11, respectively.

TABLE I. Energy-integrated cross sections in units of 10^{-20} eV cm^2.

v[a] ↓ \ v'[b] →	4	5	6	7	8	9	10	11
1	X[c]	1.0	3.8	8.13				
2	X	X	X	0.64	1.89			
3	X	X	X	X	0.11	0.34		
4	X	X	X	X	X	X	0.2	0.33

[a] v: vibrational quantum numbers of O_2.
[b] v': vibrational quantum numbers of O_2^-.
[c] X: energetically inaccessible.

and they therefore measured the convolution of the first two spikes of each level and the electron-beam energy spread. The separation between such peaks is approximately equal to twice the spacing of the vibrational levels of the compound state, i.e., 0.2 eV. The data of Schulz and Dowell can be duplicated almost exactly in the present experiment by deliberately broadening the electron energy spread.

No detailed study of the $^1\Delta_g$ and $^1\Sigma_g$ electronic states has been made in these experiments. Figure 4 shows that up to the well depths used, there is no enhancement of the trapped-electron current at the energy corresponding to the $^1\Delta_g$ state, compared with $v = 4$. It is thus confirmed that the cross section of the $^1\Delta_g$ state is very small ($\sim 10^{-20}$ cm^2) at energies up to about 150 mV above threshold.

When one attempts to compare the present vibrational excitation cross sections with those obtained from swarm experiments, the process is fraught with difficulties. It is possible that a compound state can decay into any of the energetically allowed vibrational states of the neutral molecule with the ejection of the electron. Hake and Phelps had no theoretical or experimental data for these branching ratios, and they therefore assigned the total magnitude of their resonant-type cross sections to the vibrational state just below the resonance. It can be seen from Fig. 2 that, contrary to the above assumption, compound states in O_2 show a preference for decay into the lowest possible state of the neutral molecule. As pointed out by Herzenberg, this is to be expected from theoretical considerations.[25]

The branching ratio for the decay of compound states is governed by the overlap of the appropriate wave functions and also by the probability for barrier penetration. The potential barrier involved here is that resulting from the "centrifugal" potential. The barrier penetration depends on the energy of the electrons which must escape in the decay process $O_2^- \rightarrow O_2(v) + e$. When the ratio of electron energies of the emitted electrons is large, the branching ratio also becomes large. For *d*-

wave scattering, which is involved in the reaction given above, the barrier penetration is proportional, to the first approximation,[26] to $E^{5/2}$, where E is the energy of the ejected electrons. These considerations account, in a qualitative way, for the large branching ratios shown in Fig. 2. The O_2^- ($v'=7$) state decays into O_2 ($v=1$) and O_2 ($v=2$) in the ratio of 13 : 1. The O_2^- ($v'=8$) state decays into O_2 ($v=2$) and O_2 ($v=3$) in the ratio of 17 : 1. Because of the near coincidence of the $v'=8$ level of O_2^- and the $v=3$ level of O_2, the ratio of electron energies of the ejected electrons is especially large, leading to a large branching ratio for $v=3$ and $v=2$ of O_2. It should be noted that the branching ratio for low-lying vibrational states in N_2 is close to unity.[2] This results from the fact that the ratio of energies of the ejected electrons is also close to unity since the compound state in N_2 is located near 2.3 eV and the spacing of vibrational levels is about 0.3 eV. Thus the barrier penetration in N_2 does not differ much for the decay channels leading to the low vibrational states.

When we extrapolate the vibrational spacing of the O_2^- system from the region in which it can be measured in the present experiment, and terminate the extrapolation at the value nearest to Pack and Phelps's value for the electron affinity of O_2, we obtain a value of 132 mV for the spacing of the lowest vibrational states ($v'=0 \rightarrow v'=1$) of O_2^-. This value should be compared with a value of 135 mV deduced by Holzer *et al.*[27] from Raman spectroscopy of alkali-halide crystals, in which O_2^- is trapped. The agreement between these two values is impressive.

ACKNOWLEDGMENTS

The authors are grateful to their colleagues in the Department of Engineering and Applied Science, particularly M. J. W. Boness, P. D. Burrow, A. Herzenberg, and A. Stamatovic for advice on many aspects of the present experiment. Thanks are due to A. V. Phelps for fruitful discussions and comments, and to J. H. Kearney for technical assistance.

---

†Work supported by ARPA through the Office of Naval Research and by DASA through the Army Research Office, Durham.

[1]For recent reviews, see A. V. Phelps, Rev. Mod. Phys. 40, 399 (1968); J. N. Bardsley and F. Mandl, Rept. Progr. Phys. 31, 471 (1968).

[2]G. J. Schulz, Phys. Rev. 135, A988 (1964).

[3]H. Ehrhardt, L. Langhans, F. Linder, and H. S. Taylor, Phys. Rev. 173, 222 (1968).

[4]G. J. Schulz and R. K. Asundi, Phys. Rev. 158, 25 (1967).

[5]F. R. Gilmore, J. Quant. Spectry. Radiative Transfer 5, 369 (1965).

[6]L. M. Chanin, A. V. Phelps, and M. A. Biondi, Phys. Rev. 128, 219 (1962).

[7]G. J. Schulz and J. T. Dowell, Phys. Rev. 128, 174 (1962).

[8]R. D. Hake, Jr., and A. V. Phelps, Phys. Rev. 158, 70 (1967).

[9]M. J. W. Boness and J. B. Hasted, Phys. Letters 21, 526 (1966).

[10]D. Spence and G. J. Schulz, Phys. Rev. 188, 280 (1969).

[11]R. E. Fox, W. M. Hickam, D. J. Grove, and T. Kjeldaas, Rev. Sci. Instr. 26, 1101 (1955).

[12]G. J. Schulz, Phys. Rev. 112, 150 (1958); 116, 1141 (1959).

[13]P. D. Burrow and G. J. Schulz, Phys. Rev. 187, 97 (1969).

[14]P. J. Chantry, Rev. Sci. Instr. 40, 884 (1969).

[15]Although Boness and Hasted (Ref. 9) used a transmission method in which both elastic and inelastic processes could contribute to the observed structure, we find that the inelastic cross sections are much smaller than the elastic cross section. Thus the observed structure in the transmission experiment results from the shape of the elastic cross section.

[16]M. J. W. Boness and G. J. Schulz (unpublished).

[17]G. J. Schulz, Phys. Rev. Letters 10, 104 (1963).

[18]The absolute value of the structure in the elastic cross section is obtained by normalization to the data given by H. S. W. Massey, E. H. S. Burhop, and H. B. Gilbody, in *Electronic and Ionic Impact Phenomena* (Clarendon Press, Oxford, 1968, Vol. II, p. 699. The vibrational spacing of O_2 is obtained from G. Herzberg, *Molecular Spectra and Molecular Structure* (Van Nostrand, Princeton, N. J., 1950), Vol. I, p. 560.

[19]J. A. D. Stockdale, R. N. Compton, G. S. Hurst, and P. W. Reinhardt, Jr., J. Chem. Phys. 50, 2176 (1969). These authors obtain a value in excess of 1.1 eV for the electron affinity of O_2 by measuring the appearance potential of O_2^- in the reaction $e + NO_2 \rightarrow O_2^- + N$. It is now known, however, that thermal population of vibrational and rotational states often lowers the appearance potential [see Ref. 10 and, also, G. J. Schulz and D. Spence, Phys. Rev. Letters 22, 47 (1969)], leading to an erroneously high value of the electron affinity.

[20]D. Vogt, B. Hauffe, and H. Neuert, Z. Physik 232, 439 (1970) studies the shape of the charge transfer reactions $H^- + O_2 \rightarrow H + O_2^-$ and $SO^- + O_2 \rightarrow SO + O_2$ and they deduce from the shape of the cross section in the energy range 3–80 eV that these reactions are exothermic. Since the electron affinity of H is 0.77 eV and that of SO is 1.05 eV, they deduce that the electron affinity of O_2 is larger than 1.05 eV (but smaller than 1.2 eV). However, at thermal energies the prominent reaction is $H^- + O_2 \rightarrow HO_2 + e$, i.e., associative detachment. [See F. C. Fehsenfeld, A. L. Schmeltkopf, D. B. Dunkin, and E. E. Ferguson, U.S. Department of Commerce, ESSA Technical Report No. ERL 135-AL3 (unpublished).] The rate constant for associative detachment is large, i.e., about 10^{-9} cm^3 sec^{-1}. This would indicate the existence of a short-lived compound state HO_2^- as an intermediate stage for the reaction $H^- + O_2 \rightarrow HO_2 + e$. D. Vogt [Int. J. Mass. Spectrom. Ion Phys. 3, 81 (1969)] deduces from a measurement of the angu-

lar distribution that no compound states are involved in the low-energy ion-molecule reactions. However, the angular distribution may be an insufficient guide for such a deduction since compound states can have very short lifetimes ($\sim 10^{-15}$ sec) and the angular distribution of the heavy particles may not be affected in such a case. Thus, compound states and curve hopping could contribute to the reactions. It is not clear at this time whether the shape of the charge transfer cross section in the range 3–80 eV is a reliable guide for determining electron affinities when both associative detachment and charge transfer are present. Certainly the theoretical basis for such deductions is sparse at the present time.

[21]J. L. Pack and A. V. Phelps, J. Chem. Phys. 44, 1870 (1966).
[22]I. S. Buchelnikova, Zh. Experim. i Teor. Fiz. 35, 1110 (1953) [Soviet Phys. JETP 35, 783 (1959)].
[23]G. J. Schulz, Phys. Rev. 128, 178 (1962).
[24]D. Rapp and D. D. Briglia, J. Chem. Phys. 43, 1480 (1965).
[25]A. Herzenberg (private communication).
[26]J. M. Blatt and V. F. Weisskopf, *Theoretical Nuclear Physics* (Wiley, New York, 1952), p. 360.
[27]W. Holzer, W. F. Murphy, H. J. Bernstein, and J. Rolfe, J. Mol. Spectry. 26, 543 (1968).

PHYSICAL REVIEW A VOLUME 2, NUMBER 5 NOVEMBER 1970

On the Application of Faddeev Equations and the Coulomb t Matrix to Asymptotic Electron Capture in Hydrogen†

C. P. Carpenter* and T. F. Tuan
Physics Department, University of Cincinnati, Cincinnati, Ohio 45221
(Received 9 February 1970)

Faddeev equations together with the Coulomb t matrix have been used to determine the asymptotic amplitude for electron capture from neutral hydrogen by fast protons. The results show that in the high-energy limit the capture cross section should go down as v^{-11}, where v is the velocity of the incident proton. The capture amplitude is identical to Drisko's second-Born-approximation calculation except for a complex energy-dependent phase factor which ultimately approaches unity with sufficiently high incident energy. The major contribution to the three-body capture amplitude can be shown to come from the on-energy-shell two-body t matrix, in agreement with general theorems concerning scattering from complex systems. At high incident energies, the on-energy-shell contribution to the capture amplitude (not the cross section) will decrease as v^{-5}, while the off-energy-shell continuum contribution will decrease as v^{-6}. The contributions from the sum of the infinite number of two-body bound-state poles can be shown to converge, and the sum can be explicitly performed at high enough incident energies in all except the forward direction. The bound-state contributions to the capture amplitude go down as v^{-11}, which is much less than the continuum contributions.

I. INTRODUCTION

Most of the recent investigations in the asymptotic behavior of electron-capture cross section from hydrogen at high energies involve the use of either some kind of Born and distorted-wave approximation[1–3] or the impulse approximation.[4] The approximations usually consist of a Neumann type of iteration of an integral equation whose kernel contains disconnected diagrams. Moreover, the convergence of the Born series for rearrangement three-body scattering has long been questioned.[5]

It is the purpose of the present paper to investigate the asymptotic behavior of electron capture with Faddeev's equations.[6] Other than the obvious advantage that the kernel of this equation does not contain disconnected diagrams and an iteration of such an equation may well converge in the same sense that a Born series converges for sufficiently high incident energies in two-body scattering, there is the additional advantage that the Coulomb two-body t matrix[7] is known in closed form. We shall make use of some of the high-energy-approximation techniques developed by Drisko[1] for the Born series which also happen to be applicable to the Faddeev series. To be specific, we shall consider the following reaction at high incident energies:

$$p + \mathrm{H}(1s) \rightarrow \mathrm{H}(1s) + p\,. \tag{1}$$

In the following, we will develop the general formulation and introduce the coordinate system as well as the notation in Sec. II. We shall use Lovelace's[8] formulation for the three-body scattering, which is more convenient for our purpose than the original Faddeev[6] equations. In order to facilitate comparison with previous results for the reader, we shall use the same notation as those used by Lovelace,[8] by Drisko,[1] and by Mapleton[3] wherever possible. The actual integral equation used, as well as the series expansion, will also be